

## **LOG-AMPLITUDE VARIANCE OF LASER BEAM PROPAGATION ON THE SLANT PATH THROUGH THE TURBULENT ATMOSPHERE**

**H.-Y. Wei**

Department of Physics and Optoelectronics  
Taiyuan University of Technology  
Taiyuan 030024, China

**Z.-S. Wu**

School of Science  
Xidian University  
Xi'an 710071, China

**Q.-L. Ma**

Department of Physics and Optoelectronics  
Taiyuan University of Technology  
Taiyuan 030024, China

**Abstract**—Based on the altitude-dependent model of ITU-R slant atmospheric turbulence structure constant, the log-amplitude variance of laser beam propagation on the slant path through turbulent atmosphere is obtained with transmitter and receiver parameters and can be degenerated to the result of the horizontal path with atmospheric structure constant as a fixed value. These expressions are convenient tools for beam-wave analysis. Finally, we apply the ITU-R turbulence structure constant model to calculate collimated, divergent and convergent beam log-amplitude variance. The numerical conclusions indicate the log-amplitude variance of laser beam propagation on slant path is generally smaller than those on horizontal path.

## 1. INTRODUCTION

Recently, because of the requirement of atmospheric communication, detection and remote sensing, the characteristics of the laser beam propagation on slant path become very important. The fluctuation characteristics of the amplitude and phase of an optical wave propagating through a turbulent medium have been a source of theoretical and experimental investigations for many years [1–9]. There are also many other correlative researches [10–25]. Ishimaru [1] used spectral analysis techniques to obtain expressions for the covariance and structure functions of log-amplitude and phase in locally homogeneous and isotropic turbulence. Kerr and Eiss [4] and Kerr and Dunphy [5] later demonstrated that the predicted reduction in the scintillation for a large-aperture focused beam is of limited practical significance, since it depends critically on the focus adjustment and on beam wander. Miller et al. [9] discussed the log-amplitude variance and wave structure function of Gaussian beam propagation on the horizontal path.

All the theoretical studies have centered on the horizontal path. This paper discusses the slant transmitted path. The bulk of the theoretical studies has centered on the spherical or infinite plane-wave forms, which are primarily limiting cases of more general optical propagation modes. It is difficult to interpret basic beam-wave behavior and produce numerical results with expressions left in this form. Most results for the log-amplitude variance, for example, are in the form of complicated relations, often involving functions with complex arguments. In many applications, however, neither the spherical nor the plane-wave approximation is sufficient to characterize propagation properties of the wave. In such cases it is necessary to account for beam size as well as for the focusing or diverging characteristics of the beam propagation on the slant path.

Based on the altitude-dependent model of the ITU-R turbulence structure constant model  $C_n^2(h)$ , this paper derives the log-amplitude of the laser beam propagation through atmospheric turbulence on the slant path and can be degenerated to the result of the horizontal path with atmospheric structure constant a fixed value. Finally, different Gaussian beam log-amplitude variances are calculated based on ITU-R turbulence structure constant model. In computation, because the atmospheric structure constant changes with the propagation path, the computing formulas have to reserve the  $C_n^2(h)$  path integral calculus form.

## 2. NON-DIMENSIONAL BEAM PARAMETERS

The electric field  $U$  of laser beam as to paraxial beam in the plane of the transmitter at  $z = 0$  may be written in the form

$$U(0, \rho_0) = \exp \left[ -\frac{1}{2} (k\alpha) \rho_0^2 \right] \quad (1)$$

where  $\alpha = \lambda/\pi W_0^2 + i(1/F_0)$  is the transmitter at  $z = 0$ ;  $W_0$  is the half width of initial beam;  $F_0$  is radius of curvature of wave front; and  $\rho_0$  is the coordinate of  $z = 0$ .  $\lambda$  is wave length, and  $k$  is the wave number.

Introduced non-dimensional parameters  $\Theta_0$  and  $\Lambda_0$  [9] are

$$\Theta_0 = 1 - \frac{L}{F_0}, \quad \Lambda_0 = \frac{2L}{kW_0^2} \quad (2)$$

Alternatively, one can express the complex amplitude  $1 + i\alpha L$  as the sum of real and imaginary parts, which leads to [9]

$$\begin{aligned} 1 + i\alpha L &= 1 + i\lambda L/\pi W_0^2 - (L/F_0) = \Theta_0 + i\Lambda_0 \\ 1/(1 + i\alpha L) &= 1/(\Theta_0 + i\Lambda_0) = \Theta - i\Lambda \end{aligned} \quad (3)$$

When the beam propagates from  $\vec{\rho}_0(z = 0)$  to  $\vec{\rho}(z = L)$  along  $z$  axis, the wave field at  $z = L$  (receiver) can be represented by

$$\begin{aligned} U(L, \rho) &= \frac{1}{1 + i\alpha L} \exp \left[ ikL - \frac{1}{1 + i\alpha L} \left( \frac{1}{W^2} + i\frac{k}{2F} \right) \rho^2 \right] \\ &= \frac{1}{1 + i\alpha L} \exp \left[ ikL - \left( \frac{1}{W^2} + i\frac{k}{2F} \right) \rho^2 \right] \end{aligned} \quad (4)$$

where  $F$  and  $W$  are the radius of curvature of wave front and beam half width of receiver, respectively.

$$F = \frac{F_0(\Theta_0^2 + \Lambda_0^2)(\Theta_0 - 1)}{\Theta_0^2 + \Lambda_0^2 - \Theta_0}, \quad W = W_0(\Theta_0^2 + \Lambda_0^2)^{1/2} \quad (5)$$

The parameters  $\Theta$  and  $\Lambda$  are related to  $F$  and  $W$ , expressed by

$$\Theta = \frac{\Theta_0}{\Theta_0^2 + \Lambda_0^2} = 1 + \frac{L}{F}, \quad \Lambda = \frac{\Lambda_0}{\Theta_0^2 + \Lambda_0^2} = \frac{2L}{kW^2} \quad (6)$$

The field intensity of receiver is

$$I(L, \rho) = |U(L, \rho)|^2 = \frac{W_0^2}{W^2} \exp \left( -\frac{2\rho^2}{W^2} \right) \quad (7)$$

### 3. LOG-AMPLITUDE VARIANCE OF LASER BEAM PROPAGATION ON THE SLANT PATH

If a normal distribution is assumed for the probability density of the logarithm of the beam fluctuating amplitude, the log-amplitude variance for a laser beam after propagation along a path of length  $L$  in a turbulent atmosphere is described by [9]

$$\sigma_x^2(L, \rho) = 2\pi^2 \int_0^L \int_0^\infty \left\{ I_0(2\gamma_i \kappa \rho) |H(\kappa, \rho)|^2 + \text{Re}[H^2(\kappa, z)] \right\} \Phi_n(\kappa) \kappa d\kappa dz \quad (8)$$

where  $I_0(\chi)$  is the modified Bessel function of the first kind.  $\gamma$  is the transfer constant,  $\gamma = 1$  when the wave is the plane wave, while  $\gamma = z/L$  wherever the wave is sphere wave. When the beam is laser beam, the transfer constant  $\gamma$  being complex, can be expressed as

$$\gamma = \frac{1 + i\alpha z}{1 + i\alpha L} = \gamma_r - i\gamma_i, \quad \gamma_r = \frac{1 + \alpha^2 L z}{1 + \alpha^2 L^2}, \quad \gamma_i = \frac{\alpha(L - z)}{1 + \alpha^2 L^2} \quad (9)$$

$\Phi_n(\kappa)$  in Eq. (8) is the air refraction index power spectrum;  $\kappa$  is spatial wave number;  $z$  is propagation distance

$$|H(\kappa, z)|^2 = k^2 \exp \left[ -\frac{\gamma_i \kappa^2 (L - z)}{k} \right] \quad (10)$$

$$H^2(\kappa, z) = -k^2 \exp \left[ -\frac{\gamma \kappa^2 (L - z)}{k} \right] \quad (11)$$

Taking  $\xi = z/L$  and using the receiver parameters  $\Lambda$  and  $\Theta$ , the Eq. (8) takes a simpler form

$$\begin{aligned} \sigma_x^2(L, \rho) = & 2\pi^2 k^2 L \int_0^1 \int_0^\infty \left\{ I_0(2\Lambda \rho \xi \kappa) - \cos \left[ \frac{L\kappa^2}{k} (1 - \bar{\Theta}\xi) \right] \right\} \\ & \times \left[ \exp \left( -\frac{\Lambda L \xi^2 \kappa^2}{k} \right) \right] \Phi_n(\kappa) \kappa d\kappa d\xi \end{aligned} \quad (12)$$

where the complementary parameter is

$$\bar{\Theta} = 1 - \Theta \quad (13)$$

It is useful to express the log-amplitude variance [Eq. (12)] further as the sum

$$\sigma_x^2(L, \rho) = \sigma_{x,l}^2(L) + \sigma_{x,r}^2(L, \rho) \quad (14)$$

where  $\sigma_{x,l}^2(L)$  and  $\sigma_{x,r}^2(L, \rho)$  are called the longitudinal and radial components, respectively. These components are defined by

$$\sigma_{x,l}^2(L) = 4\pi^2 k^2 L \int_0^1 \int_0^\infty \sin^2 \left[ \frac{L\kappa^2}{2k} (1 - \bar{\Theta}\xi) \right] \exp \left( -\frac{\Lambda L \xi^2 \kappa^2}{k} \right) \Phi_n(\kappa) \kappa d\kappa d\xi \quad (15)$$

$$\sigma_{x,r}^2(L, \rho) = 2\pi^2 k^2 L \int_0^1 \int_0^\infty [I_0(2\Lambda\rho\xi\kappa) - 1] \exp\left(-\frac{\Lambda L \xi^2 \kappa^2}{k}\right) \Phi_n(\kappa) \kappa d\kappa d\xi \tag{16}$$

Note that the radial component [Eq. (16)] vanishes along the beam axis  $\rho = 0$ , since  $I_0(0) = 1$ . Also, the radial component directly involves only the Fresnel ( $\rho/W$ ) ratio at the receiver  $\Lambda$ , while the longitudinal component [Eq. (15)] involves both  $\Lambda$  and curvature parameter  $\Theta$  (or  $\Theta$ ).

If optical turbulence is homogeneous along the propagation path, and the inner scale is sufficiently small with respect to the size of the Fresnel zone, the evaluation of integrals (15) and (16) can be based on the Kolmogorov spectrum

$$\Phi_n(\kappa) = 0.033 C_n^2 \kappa^{-11/3} \tag{17}$$

where  $C_n^2$  is the refractive-index structure parameter. This paper discusses the laser beam propagation on the slant path, and  $C_n^2$  is altitude dependent. Kolmogorov spectrum can be written as

$$\Phi_n(\kappa) = 0.033 C_n^2(\xi H) \kappa^{-11/3} \tag{18}$$

where  $H$  is the vertical height of receiver from ground. There we employ ITU-R atmospheric turbulence structure constant model [26] expressed by

$$C_n^2(h) = 8.148 \times 10^{-56} v_{RMS}^2 h^{10} e^{-h/1000} + 2.7 \times 10^{-16} e^{-h/1500} + C_0 e^{-h/100} \tag{19}$$

where  $v_{RMS} = \sqrt{v_g^2 + 30.69v_g + 348.91}$  is the wind velocity of vertical path;  $v_g$  is sub aerial wind velocity;  $C_0$  is sub aerial atmospheric structure constant (its typical value is  $1.7 \times 10^{-14} m^{-2/3}$ ).

Substituting Eq. (18) into Eq. (16), then

$$\begin{aligned} \sigma_{x,r}^2(L, \rho) &= 0.066\pi^2 k^2 L \int_0^1 C_n^2(\xi H) d\xi \\ &\times \int_0^\infty [I_0(2\Lambda\rho\xi\kappa) - 1] \exp\left(-\frac{\Lambda L \xi^2 \kappa^2}{k}\right) \kappa^{-8/3} d\kappa \end{aligned} \tag{20}$$

The result of integrand Eq. (20) is

$$\begin{aligned} \sigma_{x,r}^2(L, \rho) &= 0.033\pi^2 C_{n0}^2 k^{7/6} L^{11/6} \Gamma(-5/6) \Lambda^{5/6} \\ &\times \int_0^1 \frac{C_n^2(\xi H)}{C_{n0}^2} \xi^{5/3} [{}_1F_1(-5/6; 1; 2\rho^2/W^2) - 1] d\xi \end{aligned} \tag{21}$$

Reducing Eq. (21)

$$\sigma_{x,r}^2(L, \rho) = 1.77\sigma_0^2 \Lambda^{5/6} [1 - {}_1F_1(-5/6; 1; 2\rho^2/W^2)] \int_0^1 \frac{C_n^2(\xi H)}{C_{n0}^2} \xi^{5/3} d\xi \tag{22}$$

where  $\sigma_0^2 = 1.23C_{n0}^2k^{7/6}L^{11/6}$  is the Rytov covariance. The atmospheric turbulence structure constant on the slant path is a fixed value  $C_n^2(\xi H) = C_{n0}^2$  Eq. (22) can be degenerated to the result of the horizontal path

$$\begin{aligned} \sigma_{x,r}^2(L, \rho) &= 1.77\sigma_0^2\Lambda^{5/6} [1 - {}_1F_1(-5/6; 1; 2\rho^2/W^2)] \int_0^1 \xi^{5/3} d\xi \\ &= 0.66\sigma_0^2\Lambda^{5/6}[1 - {}_1F_1(-5/6; 1; 2\rho^2/W^2)] \end{aligned} \tag{23}$$

where  ${}_1F_1(a; c; x)$  is the hypergeometric function of the first kind [27]. For  $\rho \leq W$  the radial component [Eq. (23)] can be closely approximated with the first few terms of the series representation of the  ${}_1F_1$ , whereas the large-argument asymptotic form of  ${}_1F_1$  may be used for large values of  $\rho/W$ . The result of these approximations is

$$\sigma_{x,r}^2(L, \rho) \approx \begin{cases} 1.1\sigma_0^2\Lambda^{5/6}(\rho/W)^2[1 + 0.083(\rho/W)^2] & \rho \leq W \\ 0.027\sigma_0^2\Lambda^{5/6}(\rho/W)^{11/3} \exp(2\rho^2/W^2) & \rho \gg W \end{cases} \tag{24}$$

Hence, when  $\rho < W$ , radial component (23) increases approximately as the square of the distance from the center line of the beam to the diffractive beam radius at the receiver [ignoring the small contribution from the multiplicative factor  $1 + 0.083(\rho/W)^2$ ]. For  $\rho \gg W$  the radial component predicts a rapid increase with  $\rho$ , owing to the exponential behavior of the  ${}_1F_1$  function.

We can express the longitudinal component Eq. (15) as

$$\begin{aligned} \sigma_{x,l}^2(L) &= 2\pi^2k^2L \int_0^1 \int_0^\infty \Phi_n(\kappa)\kappa \left\{ 1 - \cos \left[ \frac{L\kappa^2}{k} (1 - \bar{\Theta}\xi)\xi \right] \right\} \\ &\quad \exp \left( -\frac{\Lambda L\xi^2\kappa^2}{k} \right) d\kappa d\xi \end{aligned} \tag{25}$$

Using Eq. (18)

$$\begin{aligned} \sigma_{x,l}^2(L) &= 2\pi^2k^2L \int_0^1 0.033C_n^2(\xi H) d\xi \\ &\quad \times \int_0^\infty \left\{ 1 - \cos \left[ \frac{L\kappa^2}{k} (1 - \bar{\Theta}\xi)\xi \right] \right\} \exp \left( -\frac{\Lambda L\xi^2\kappa^2}{k} \right) \kappa^{-8/3} d\kappa \end{aligned} \tag{26}$$

The result of integrand is

$$\begin{aligned} \sigma_{x,l}^2(L) &= 0.033\Gamma(-5/6)\pi^2C_{n0}^2k^{7/6}L^{11/6} \int_0^1 \frac{C_n^2(\xi H)}{C_{n0}^2} \\ &\quad \times \left\{ \Lambda^{5/6}\xi^{5/3} - [\Lambda^2\xi^4 + (1 - \bar{\Theta}\xi)^2\xi^2]^{5/12} \right. \\ &\quad \left. \cos \left[ \frac{5}{6} \tan^{-1} \left( \frac{1 - \bar{\Theta}\xi}{\Lambda\xi} \right) \right] \right\} d\xi \end{aligned} \tag{27}$$

Equation (27) is simplified as

$$\begin{aligned} \sigma_{x,l}^2(L) &= 1.77\sigma_0^2 \int_0^1 \frac{C_n^2(\xi H)}{C_{n0}^2} \\ &\quad \times \left\{ [\Lambda^2 \xi^4 + (1 - \bar{\Theta}\xi)^2 \xi^2]^{5/12} \cos \left[ \frac{5}{6} \tan^{-1} \left( \frac{1 - \bar{\Theta}\xi}{\Lambda \xi} \right) \right] \right. \\ &\quad \left. - \Lambda^{5/6} \xi^{5/3} \right\} d\xi \end{aligned} \tag{28}$$

When atmospheric turbulence structure constant is a fixed value  $C_n^2(\xi H) = C_{n0}^2$ , Eq. (28) can be degeneracy as the result of laser beam propagation on the horizontal path

$$\begin{aligned} \sigma_{x,l}^2(L) &= 1.77\sigma_0^2 \int_0^1 \left\{ [\Lambda^2 \xi^4 + (1 - \bar{\Theta}\xi)^2 \xi^2]^{5/12} \cos \left[ \frac{5}{6} \tan^{-1} \left( \frac{1 - \bar{\Theta}\xi}{\Lambda \xi} \right) \right] \right. \\ &\quad \left. - \Lambda^{5/6} \xi^{5/3} \right\} d\xi = 0.66\sigma_0^2 \left[ f(\bar{\Theta}, \Lambda) - \Lambda^{5/6} \right] \end{aligned} \tag{29}$$

where

$$f(\bar{\Theta}, \Lambda) = \text{Re}[(16/11)i^{5/6} {}_2F_1(-5/6, 11/6, 17/6; \bar{\Theta} + i\Lambda)] \tag{30}$$

And  ${}_2F_1(a, b, c; \chi)$  is the hypergeometric function. Submitting Eq. (22) and Eq. (28) into Eq. (14), we can obtain log-amplitude variance of beam propagation on the slant path

$$\begin{aligned} \sigma_x^2(L, \rho) &= 1.77\sigma_0^2 \Lambda^{5/6} \int_0^1 \frac{C_n^2(\xi H)}{C_{n0}^2} \xi^{5/3} d\xi \left\{ [1 - {}_1F_1(-5/6; 1; 2\rho^2/W^2)] \right. \\ &\quad \left. + [\Lambda^2 \xi^4 + (1 - \bar{\Theta}\xi)^2 \xi^2]^{5/12} \cos \left[ \frac{5}{6} \tan^{-1} \left( \frac{1 - \bar{\Theta}\xi}{\Lambda \xi} \right) \right] - \xi^{5/3} \right\} \end{aligned} \tag{31}$$

Submitting Eq. (23) and Eq. (29) into Eq. (14), we can obtain log-amplitude variance of beam propagation on the horizontal path

$$\sigma_x^2(L, \rho) = 0.66\sigma_0^2 \left[ f(\bar{\Theta}, \Lambda) - \Lambda_1^{5/6} {}_1F_1(-5/6; 1; 2\rho^2/W^2) \right] \tag{32}$$

It is equivalent to the result that Ishimaru [28] obtained. Simplifying Eq. (30) to more tractable analytic functions depends on the particular beam form. For instance, it can readily be shown that  $|\bar{\Theta} + i\Lambda| \leq 1$  when  $\Theta_0 \geq 0.5$ , which corresponds to all divergent and collimated beam forms and some convergent beams. In this case the series representation of the hypergeometric function in Eq. (30) yields

$$\begin{aligned} f(\bar{\Theta}, \Lambda) &= \frac{11}{16} \sum_{n=0}^{\infty} \frac{(-5/6)_n (11/6)_n}{(17/6)_n n!} (\bar{\Theta}^2 + \Lambda^2)^{n/2} \cos \left[ n \tan^{-1} \left( \frac{\Lambda}{\bar{\Theta}} \right) + \frac{5\pi}{12} \right], \\ &\quad |\bar{\Theta} + i\Lambda| \leq 1 \end{aligned} \tag{33}$$

where  $(a)_n = \Gamma(a + n)/\Gamma(a)$ ,  $n = 0, 1, 2, 3, \dots$

Also,  $|\bar{\Theta} + i\Lambda| > 1$  wherever  $\Theta_0 < 0.5$ , and one may then use the analytic continuation formula

$$\begin{aligned}
 {}_2F_1(a, b, c; -x) &= \frac{\Gamma(c)\Gamma(b-a)}{\Gamma(b)\Gamma(c-a)} x^{-a} {}_2F_1(a, 1+a-c, 1+a-b; -1/x) \\
 &\quad + \frac{\Gamma(c)\Gamma(a-b)}{\Gamma(a)\Gamma(c-b)} x^{-b} {}_2F_1(b, 1+b-c, 1+b-a; -1/x) \quad (34)
 \end{aligned}$$

For the hypergeometric function in Eq. (30) to obtain the representation

$$\begin{aligned}
 f(\bar{\Theta}, \Lambda) &= 0.338(\bar{\Theta}^2 + \Lambda^2)^{-11/12} \cos \left[ \frac{11}{6} \tan^{-1} \left( \frac{\Lambda}{\bar{\Theta}} \right) - \frac{\pi}{4} \right] + (\bar{\Theta}^2 + \Lambda^2)^{5/12} \\
 &\quad \times \sum_{n=0}^{\infty} \frac{(-5/6)_n (11/6)_n}{(17/6)_n n!} (\bar{\Theta}^2 + \Lambda^2)^{-n/2} \cos \left[ \left( n - \frac{5}{6} \right) \tan^{-1} \left( \frac{\Lambda}{\bar{\Theta}} \right) + \frac{5\pi}{12} \right], \\
 &\quad |\bar{\Theta} + i\Lambda| > 1 \quad (35)
 \end{aligned}$$

### 3.1. Collimated Beam

For a collimated beam the parameters  $\Lambda$  and  $\Theta$  are completely determined by  $\Lambda_0$ , since  $\Theta_0 = 1$  for this beam type. Also, Eq. (33) can be used for  $f(\Theta, \Lambda)$  in the longitudinal component Eq. (29), since  $|\bar{\Theta} + i\Lambda| \leq 1$ . Writing both  $\Theta$  and  $\Lambda$  in terms of  $\Lambda_0$ , we arrive at the expression

$$\begin{aligned}
 \frac{\sigma_{x,l}^2(L)}{\sigma_0^2} &= 0.96 \sum_{n=0}^{\infty} \frac{(-5/6)_n (11/6)_n}{(17/6)_n n!} \left( \frac{\Lambda_0^2}{1 + \Lambda_0^2} \right)^{n/2} \cos \left[ n \tan^{-1} \left( \frac{1}{\Lambda_0} \right) + \frac{5\pi}{12} \right] \\
 &\quad - 0.66 \left( \frac{\Lambda_0}{1 + \Lambda_0^2} \right)^{5/6} \quad (36)
 \end{aligned}$$

Two linear transformations on the hypergeometric function in Eq. (30) yield the alternative form

$$\begin{aligned}
 \frac{\sigma_{x,l}^2(L)}{\sigma_0^2} &= 0.39 \left( \frac{1 + \Lambda_0^2}{\Lambda_0^2} \right)^{11/12} \sin \left[ \frac{11}{6} \tan^{-1} (\Lambda_0) \right] - 0.66 \left( \frac{\Lambda_0}{1 + \Lambda_0^2} \right)^{5/6} \\
 &\quad + 0.96 \Lambda_0^{-11/6} \sum_{n=0}^{\infty} \frac{(-5/6)_n (11/6)_n}{(17/6)_n n!} (1 + \Lambda_0^2)^{-n/2} \sin [n \tan^{-1} (\Lambda_0)] \quad (37)
 \end{aligned}$$

The series in Eq. (36) converges more rapidly than that in Eq. (37) except for large  $\Lambda_0$ , and thus Eq. (36) is generally more useful in calculations. Eqs. (36) and (37) in the limit  $\Lambda_0 = 0$  yield the standard



plane-wave expression  $\sigma_{x,p}^2 = 0.307C_n^2k^{7/6}L^{11/6}$  while producing the standard spherical-wave expression  $\sigma_{x,s}^2 = 0.124C_n^2k^{7/6}L^{11/6}$  in the limit  $\Lambda_0 = \infty$ .

The numerical results indicate that the log-amplitude variance of laser beam propagation on the slant path in the turbulent atmosphere is generally smaller than that on horizontal path. Because the drone is higher the intensity of the turbulence is weaker.

### 3.2. Divergent Beam

A divergent beam is characterized by  $\Theta_0 > 1$  with  $|\bar{\Theta} + j\Lambda| \leq 1$ , and thus we can substitute Eq. (33) into Eq. (29) to obtain

$$\frac{\sigma_{x,l}^2(L)}{\sigma_0^2} = 0.96 \sum_{n=0}^{\infty} \frac{(-5/6)_n(11/6)_n}{(17/6)_n n!} (\bar{\Theta}^2 + \Lambda^2)^{n/2} \cos \left[ n \tan^{-1} \left( \frac{\Lambda}{\bar{\Theta}} \right) + \frac{5\pi}{12} \right] - 0.66\Lambda^{5/6} \tag{38}$$

The log-amplitude variance for the divergent beam, like that for the collimated beam, tends to that of spherical wave case for decreasing beam size, since the values  $\Lambda = \Theta = 0$  are obtained in the limit  $\Lambda_0 = \infty$ . For  $\Lambda_0 \rightarrow 0$ , however, the behavior may differ from that of the collimated beam because  $\Theta$  approaches the limiting value  $\Theta = 1/\Theta_0$  rather than unity. The value of the longitudinal component moving from plane wave to spherical wave, as  $\Theta_0$  increasing from unity.

This limiting behavior is demonstrated in Fig. 1 on horizontal and in Fig. 2 on slant path. Note that the curves of divergent beam are much like those of collimated beam, except that they appear to

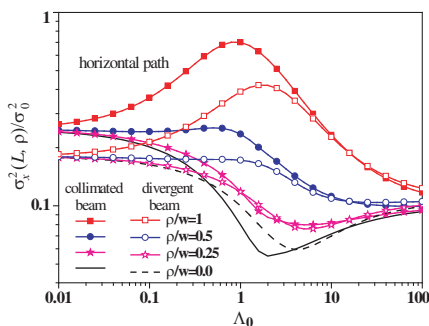


**Figure 1.** Scaled log-amplitude variance of laser beam Propagation on the horizontal path for  $\Lambda_0$  and various Fresnel ratio.

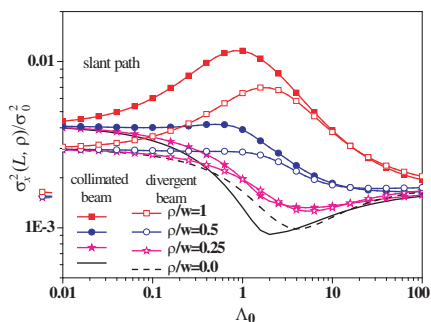


**Figure 2.** Scaled log-amplitude variance of laser beam Propagation on the slant path for  $\Lambda_0$  and various Fresnel ratio.

be shifted to the right. For example, the largest off-axis fluctuations occur near  $\Lambda_0 = 2$  rather than near unity as for collimated beam when  $\rho/W \geq 0.5$ . And the smallest value occurs near  $\Lambda_0 = 5$  when  $\rho/W < 0.5$ .

### 3.3. Convergent Beam

A convergent beam is characterized by the relation  $\Theta_0 < 1$ , and when it is compared with other beam types, exhibits some notable extremes in behavior owing to large variations in the values of  $\Lambda$  and  $\Theta$  when  $\Theta_0$  is near zero. In Figs. 3 and 4 the parameters  $\Lambda$  and  $\Theta$ , respectively, are plotted as functions of  $\Lambda_0$  for several values of  $|\Theta_0|$ . Observe that for  $\Theta_0 \neq 0$  the Fresnel ratio  $\Lambda$  approaches zero as  $\Lambda_0 \rightarrow 0$  and  $\Lambda_0 \rightarrow \infty$ , while at  $\Lambda_0 = |\Theta_0|$  it assumes its maximum value  $\Lambda_{\max} = 1/2\Theta_0$ . Only when  $\Theta_0 = 0$  the resulting Fresnel ratio  $\Lambda = 1/\Lambda_0$  becomes unbounded as  $\Lambda_0 \rightarrow 0$ . The quantity  $|\Theta|$  also approaches zero as  $\Lambda_0 \rightarrow \infty$ , but as  $\Lambda_0 \rightarrow 0$  it approaches its maximum value  $|\Theta|_{\max} = 1/|\Theta_0|$ ,  $\Lambda_0 = 0$ ,  $\Theta_0 \neq 0$ . When  $\Lambda_0 = 0$ , it follows that  $\Theta \rightarrow +\infty$  as  $\Theta_0 \rightarrow 0^+$  and  $\Theta \rightarrow -\infty$  as  $\Theta_0 \rightarrow 0^-$ .

For a convergent beam with  $0.5 \leq \Theta_0 < 1$  the analytic expression describing the longitudinal component for the log-amplitude variance has the same form as that of the divergent beam given by Eq. (38). However, when  $\Theta_0 < 0.5$ , (35) above must be used for  $f(\Theta, \Lambda)$ , which leads to

$$\begin{aligned} \frac{\sigma_{x,l}^2(L)}{\sigma_0^2} &= 0.22(\bar{\Theta}^2 + \Lambda^2) \cos \left[ \frac{11}{6} \tan^{-1} \left( \frac{\Lambda}{\bar{\Theta}} \right) - \frac{\pi}{4} \right] - 0.66\Lambda^{5/6} + 0.66(\bar{\Theta}^2 + \Lambda^2)^{5/12} \\ &\times \sum_{n=0}^{\infty} \frac{(-5/6)_n (-8/3)_n}{(-5/3)_n n!} (\bar{\Theta}^2 + \Lambda^2)^{-n/2} \cos \left[ \left( n - \frac{5}{6} \right) \tan^{-1} \left( \frac{\Lambda}{\bar{\Theta}} \right) + \frac{5\pi}{12} \right] \\ &|\bar{\Theta} + j\Lambda| > 1 \end{aligned} \quad (39)$$

For the traditional case of a perfectly focused beam defined by  $\Theta_0 = 0$ , Eq. (39) can be rewritten in the form

$$\begin{aligned} \frac{\sigma_{x,l}^2(L)}{\sigma_0^2} &= 0.22 \left( \frac{\Lambda_0^2}{1 + \Lambda_0^2} \right)^{11/12} \cos \left[ \frac{11}{6} \tan^{-1} \left( \frac{1}{\Theta\Lambda_0} \right) - \frac{\pi}{4} \right] - 0.66\Lambda^{5/6} \\ &+ 0.66 \left( \frac{1 + \Lambda_0^2}{\Lambda_0^2} \right)^{5/12} \sum_{n=0}^{\infty} \frac{(-5/6)_n (-5/6)_n}{(-5/3)_n n!} \left( \frac{\Lambda_0^2}{1 + \Lambda_0^2} \right)^{n/2} \\ &\times \cos \left[ \left( n - \frac{5}{6} \right) \tan^{-1} \left( \frac{1}{\Lambda_0} \right) + \frac{5\pi}{12} \right] \end{aligned} \quad (40)$$

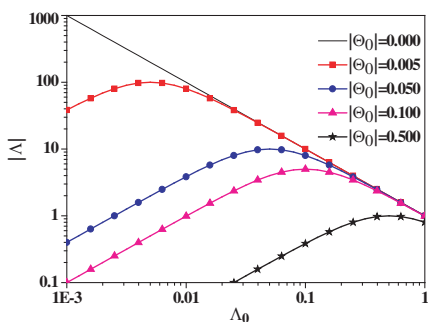


**Figure 3.** Fresnel ratio at the receiver  $\Lambda$  as a function of the Fresnel ratio at the transmitter  $\Lambda_0$  for convergent beams with various values of  $|\Theta_0|$ .

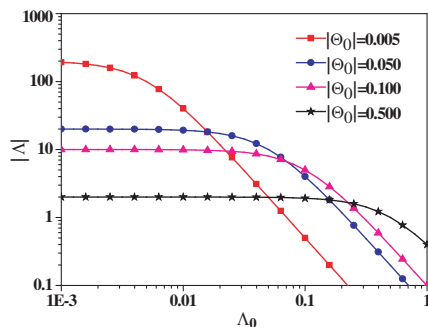


**Figure 4.** Absolute value of the receiver curvature parameter  $\Theta$  for convergent beams with various of  $\Theta_0$  as a function of the Fresnel ratio at the transmitter  $\Lambda_0$ .

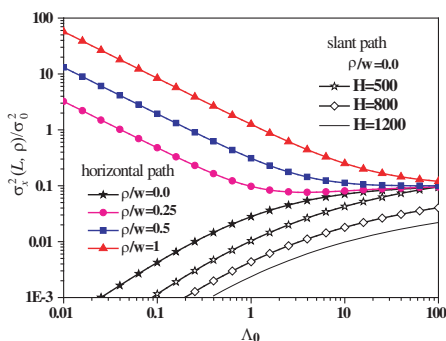


**Figure 5.** Scaled log-amplitude variance for a perfectly focused beam as a function of the Fresnel ratio at the transmitter  $\Lambda_0$  for various radial distances on the horizontal and slant path.

Consistent with other beam forms, the radial component approaches zero as  $\Lambda_0 = 0$ ; the longitudinal component approaches zero as  $\Lambda_0 = \infty$ ; and the longitudinal component approaches that of a spherical wave. However, as  $\Lambda_0 = 0$  the longitudinal component vanishes, while the radial component becomes unbounded. Fig. 5 also shows us the change relationship of scale log-amplitude variance with different heights of drone. For a fixed  $\Lambda_0$ , the higher the drone is, the smaller the log-amplitude is. With the increase of the  $H$ , the atmospheric turbulence effects become smaller and smaller.

#### 4. CONCLUDING REMARKS

Beam-wave propagation in free space can be described by wavelength, path length, transmitter beam size  $W_0$ , and radius of curvature  $F_0$ . However, when optical turbulence effects are included, the beam parameters  $W_0$  and  $F_0$  by themselves do not always lead to a clear understanding of the resulting complex phenomenon. That is, many quantities of interest are often complicated functions of  $W_0$  and  $F_0$ , from which it is difficult to discern subtle differences between behavior patterns and the various beam forms. It has been demonstrated here that beam-wave propagation in free space is also completely specified by the transmitter beam parameters  $\Lambda_0$  and  $\Theta_0$  or, equivalently, the receiver parameters  $\Lambda$  and  $\Theta$ , in addition to wavelength and path length. The receiver parameters have special physical significance, since they form the real and imaginary parts of the complex amplitude of the beam and also lead to relatively simple forms of the derived statistical quantities.

This paper discusses the relation of the log-amplitude variance of laser beam propagation through turbulent atmosphere on the slant path with transmitter and receiver parameters, and analysis optical turbulence-related characteristics predicted for Gaussian beam. These expressions are simple and can be degenerated to the result of the horizontal path with atmospheric structure constant a fixed value. All the derived analytic expressions are completely general and not bound by such restrictions.

The Kolmogorov power-law spectrum was chosen because of its simplicity but also because derived analytic forms can be degenerated to the result of the horizontal path that may be compared with earlier contributions to the field based primarily on the same spectral model. Nonetheless, it is recognized by the authors that the presence of a nonzero inner scale and a finite and the pronounced vertical nature of profiles for  $C_n^2(h)$  have important effects on optical scintillations and phase fluctuations. Thus the limiting inertial range behavior described here is valid only

- (1) the optical turbulence strength is weak to moderate
- (2) the inner scale of the turbulence is relatively small
- (3) the outer scale of the turbulence is sufficiently large
- (4) the propagation is essentially along a horizontal path.

More realistic propagation environments including saturation must eventually be considered if our understanding is to extend beyond limiting results. In this regard, research is currently under way to extend these findings to other situations involving more general spectral models and the strong-fluctuation regime.

Finally, the beam log-amplitude variance is calculated based on ITU-R turbulence structure constant model which is altitude dependent. The calculations indicate the log-amplitude variance of laser beam propagation on slant path is generally smaller than the that on horizontal path. Because the drone is higher, the intensity of the turbulence is weaker. This research is of great importance to the application of laser collimation, laser local technique and the research of laser propagation theory.

## ACKNOWLEDGMENT

This research is supported by Youth Foundation of Taiyuan University of Technology (0302064), Zhejiang Provincial Natural Science Foundation of China under grants Y (1100095), and Huzhou City Natural Science Foundation of China under grants (2010C50116).

## REFERENCES

1. Ishimaru, A., "Fluctuations of a beam wave propagating through a locally homogeneous medium," *Radio Sci.*, Vol. 4, 295–305, 1969.
2. Ho, T. L., "Log-amplitude fluctuations of a laser beam in a turbulent atmosphere," *J. Opt. Soc. Am.*, Vol. 60, 667–673, 1970.
3. Lawrence, R. S. and J. W. Strohbehn, "A survey of clear-air propagation effects relevant to optical communications," *Proc. IEEE*, Vol. 58, 1523–1545, 1970.
4. Kerr, J. R. and R. Eiss, "Transmitter-size and focus effects on scintillations," *J. Opt. Soc. Am.*, Vol. 62, 682–684, 1972.
5. Kerr, J. R. and J. R. Dunphy, "Experimental effects of finite transmitter apertures on scintillation," *J. Opt. Soc. Am.*, Vol. 63, 1–8, 1973.
6. Fante, R. L., "Electromagnetic beam propagation in turbulent media," *Proc. IEEE*, Vol. 63, 1669–1692, 1975.
7. Fante, R. L., "Electromagnetic beam propagation in turbulent media: An update," *Proc. IEEE*, Vol. 68, 1424–1443, 1980.
8. Zuev, V. E., *Laser Beams in the Atmosphere*, J. S. Wood (ed.), Trans. Consultants Bureau, New York, 1982.
9. Miller, W. B., J. C. Riclin, and L. C. Adreus, "Log-amplitude variance and wave structure function: A new perspective for Gaussian beams," *J. Opt. Soc. Am.*, Vol. 10, 661–672, 1993.
10. Georgiadou, E. M., A. D. Panagopoulos, and J. D. Kanellopoulos, "Millimeter wave pulse propagation through distorted Raindrops

- for fixed wireless access channels,” *Journal of Electromagnetic Waves and Applications*, Vol. 20, No. 9, 1235–1248, 2006.
11. Wei, H. Y. and Z. S. Wu, “Study on the effect of laser beam propagation on the slant path through atmospheric turbulence,” *Journal of Electromagnetic Waves and Applications*, Vol. 22, No. 5–6, 787–802, 2008.
  12. Wu, Z.-S., H.-Y. Wei, R.-K. Yang, and L.-X. Guo, “Study on scintillation considering inner and outer-scales for laser beam propagation on the slant path through the atmospheric turbulence,” *Progress In Electromagnetics Research*, Vol. 80, 277–293, 2008.
  13. Wei, H. Y., Z. S. Wu, and H. Peng, “Scattering from a Diffuse Target in the slant atmospheric turbulence,” *Acta Physica Sinica*, Vol. 57, No. 10, 6666–6671, 2008.
  14. Ngo Nyobe, E. and E. Pemha, “Shape optimization using genetic algorithms and laser beam propagation for the determination of the diffusion coefficient in a hot turbulent jet or air,” *Progress In Electromagnetics Research B*, Vol. 4, 211–221, 2008.
  15. Hona, J., E. Ngo Nyobe, and E. Pemha, “Experimental technique using interference pattern for measuring directional fluctuations of a laser beam created by a strong thermal turbulence,” *Progress In Electromagnetics Research*, Vol. 84, 289–306, 2008.
  16. Wang, F., Y. Cai, H. T. Eyyuboglu, and Y. K. Baykal, “Average intensity and spreading of partially coherent standard and elegant laguerre-Gaussian beams in turbulent atmosphere,” *Progress In Electromagnetics Research*, Vol. 103, 33–56, 2010.
  17. Li, J., Y. Chen, S. Xu, Y. Wang, M. Zhou, Q. Zhao, Y. Xin, and F. Chen, “Average intensity and spreading of partially coherent four-petal Gaussian beams in turbulent atmosphere,” *Progress In Electromagnetics Research B*, Vol. 24, 241–262, 2010.
  18. Kanellopoulos, J. D., A. D. Panagopoulos, and S. N. Livieratos, “Differential rain attenuation statistics including an accurate estimation of the effective slant path lengths,” *Progress In Electromagnetics Research*, Vol. 28, 97–120, 2000.
  19. Ngo Nyobe, E. and E. Pemha, “Propagation of a laser beam through a plane and free turbulent heated air flow: Determination of the stochastic characteristics of the laser beam random direction and some experimental results,” *Progress In Electromagnetics Research*, Vol. 53, 31–53, 2005.
  20. Mandeep, J. S., S. I. S. Hassan, M. F. Ain, and K. Igatashi, “Tropospheric scintillation measurement in malaysias at kuband,” *Journal of Electromagnetic Waves and Applications*, Vol. 22,

- No. 8–9, 1063–1070, 2008.
21. Zhang, Y.-Q. and Z.-S. Wu, “Character of light scattering of spatial dynamic objects at different stations and analysis of relativity,” *Journal of Electromagnetic Waves and Applications*, Vol. 22, No. 8–9, 1071–1080, 2008.
  22. Rojas, J. A. M., J. Alpuente, E. Bolivar, P. López-Espí, S. Vignote, and M. I. Rojas, “Empirical characterization of wood surfaces by means of iterative autocorrelation of laser speckle patterns,” *Progress In Electromagnetics Research*, Vol. 80, 295–306, 2008.
  23. Jandieri, G. V., A. Ishimaru, et al., “Model computations of angular power spectra for anisotropic absorptive turbulent magnetized plasma,” *Progress In Electromagnetics Research*, Vol. 70, 307–328, 2007.
  24. Ayub, M., M. Ramzan, and A. B. Mann, “A note on spherical electromagnetic wave diffraction by a perfectly conducting strip in a homogeneous bi-isotropic medium,” *Progress In Electromagnetics Research*, Vol. 85, 169–194, 2008.
  25. Apostol, M. and G. Vaman, “Plasmons and diffraction of an electromagnetic plane wave by a metallic sphere,” *Progress In Electromagnetics Research*, Vol. 98, 97–118, 2009.
  26. ITU-R. Document 3J/31-E, “On propagation data and prediction methods required for the design of space-to-earth and earth-to-space optical communication systems,” *Radio Communication Study Group Meeting*, 277–293, Budapest, 2001.
  27. Andrews, L. C., *Special Functions of Mathematics for Engineers*, 2nd edition, McGraw-Hill, New York, 1992.
  28. Ishimaru, A., *Laser Beam Propagation in the Atmosphere*, Springer, New York, 1978.